Fish and Shellfish Immunology 169 (2026) 111095

Contents lists available at ScienceDirect

Fish and Shellfish Immunology

journal homepage: www.elsevier.com/locate/fsi

Full length article

Comparative immunological study on granulocyte populations in the Leydig organ of two elasmobranch species

Giampaolo Bosi [a], Paolo Merella [b], Emanuela Franchella [c], Bahram Sayyaf Dezfuli [c], Stefania Zava [d], Paola Antonia Corsetto [d], Luisa Giari [e,*]

[a] Department of Veterinary Medicine and Animal Science, University of Milan, Università St. 6, Lodi, 26900, Italy
[b] Department of Veterinary Medicine, University of Sassari, Vienna St. 2, 07100, Sassari, Italy
[c] Department of Life Sciences and Biotechnology, University of Ferrara, Borsari St. 46, 44121, Ferrara, Italy
[d] Department of Pharmacological and Biomolecular Sciences, University of Milan, Trentacoste St. 2, 20134, Milan, Italy
[e] Department of Environmental and Prevention Sciences, University of Ferrara, Borsari St. 46, 44121, Ferrara, Italy

ARTICLE INFO

Keywords:
Leydig organ
Immune cells
Small-spotted catshark
Thornback ray
Immunohistochemistry
Granulocyte populations

ABSTRACT

Elasmobranchs are the most primitive jawed vertebrates, and their immune system is similar to those of amniotes. Therefore, sharks and rays represent excellent models for investigating the evolution of immune system components and functions. In addition to the typical lymphoid tissues, namely the thymus and spleen, elasmobranchs have Leydig (LO) and epigonal organs instead of bone marrow. The LO is located between the submucosa and muscular layers of the esophagus. Here, we report the cell composition of the LO in two elasmobranch species, the thornback ray (*Raja clavata*) and the small-spotted catshark (*Scyliorhinus canicula*). In February 2021, ten specimens of each species were collected from North Sardinia (Italy), and the esophagus was excised and studied using immunohistochemistry to characterize the immune cells in the LO. The anti-proliferating cell nuclear antigen antibody showed that approximately 44 % of cells were in DNA synthesis activity, and approximately 14 % were myeloid progenitors positive for the anti-c-kit antibody. A panel of antibodies targeting the main molecules of immune system cells was employed, showing that the LO of *R. clavata* and *S. canicula* had similar percentages of areas occupied by granulocyte types containing lysozyme, serotonin, histamine, tumor necrosis factor-like peptide, and inducible nitric oxide synthase. A comparison of the current data on these two species with previous results on the blackmouth catshark, *Galeus melastomus*, revealed some differences in the percentages of areas with granulocyte populations that express histamine, serotonin, and tumor necrosis factor-like peptide.

1. Introduction

Elasmobranchs share many features of mammalian innate and adaptive immunity, "but often in its most basic form" [1]. Studies on the immune cells of these ancient vertebrates are useful for a better understanding of early immune evolution and immune system physiology. Among jawed vertebrates, elasmobranchs are one of the most primitive groups that possess true lymphoid organs, namely the thymus, spleen, and gut-associated lymphoid tissue [2]. In addition, sharks and rays have lymphoid tissues associated with the esophagus and gonads, the Leydig organ (LO), and the epigonal organ, respectively [2]. Both organs have a lympho-myeloid structure and are equivalent to the bone marrow of amniotes [2,3], but do not differentiate erythrocytes [4]. The LO is formed by two masses of tissue located in the dorsal and ventral positions of the esophagus, between the submucosal and muscular layers, and extending from the oral cavity to the stomach [3]. Histologically, the LO is formed by lobes of mature and developing granulocytes, lymphocytes, and plasma cells contained in a stroma of fibrocytes and collagen fibers, traversed by arterioles and venules, and separated from each other by large blood lacunae [2–6].

Several ultrastructural studies on the LO of many elasmobranchs indicate that the production, differentiation, and storage of granulocytes are its main roles [3,4]. Granulocytes can be identified using Giemsa-stained smears and tissue sections. Although there is great

* Corresponding author.
E-mail addresses: giampaolo.bosi@unimi.it (G. Bosi), paolomerella@uniss.it (P. Merella), emanuela.franchella@unife.it (E. Franchella), dzb@unife.it (B. Sayyaf Dezfuli), stefania.zava@unimi.it (S. Zava), paola.corsetto@unimi.it (P.A. Corsetto), luisa.giari@unife.it (L. Giari).

https://doi.org/10.1016/j.fsi.2025.111095
Received 16 May 2025; Received in revised form 18 December 2025; Accepted 29 December 2025
Available online 30 December 2025

variability in the staining properties of granulocytes, most studies have reported three main types of granulocytes [4,7–10]: (I) cells with coarse, strongly eosinophilic granules and a simple or bi-lobed nucleus called "coarse eosinophilic granulocytes" (CEGs); (II) cells with fine eosinophilic granules and a simple or polymorphous nucleus named "fine eosinophilic granulocytes" (FEGs); and (III) neutrophilic cells lacking or with fine granules called "non-eosinophilic granulocytes" or simply "neutrophils" [9,10].

Despite the well-known histology and cells ultrastructure of the LO in elasmobranchs, we are the first to characterize and quantify the cell types in this hematopoietic site. Initial findings have documented the presence of granulocytes containing nine distinct immunological molecules in the LO of the blackmouth catshark *Galeus melastomus* [6]. In the present study, a similar array of immunological markers, as used for *G. melastomus*, was applied to the LO of the thornback ray, *Raja clavata*, and the small-spotted catshark, *Scyliorhinus canicula*, to quantify the different granulocyte population types and compare their composition in these two species.

2. Materials and methods

Ten specimens of each of *R. clavata* and *S. canicula* from the Gulf of Asinara (Sardinia, western Mediterranean Sea) were caught in February 2021 during a haul at a depth of 500–800 m from commercial trawl fishing. The catsharks weighed 197–253 g (mean total weight ± standard deviation: 231.0 ± 20.9 g), and rays weighed 104–162 g (mean total weight ± standard deviation: 141.3 ± 12.5 g). The specimens destined to the fish market were eviscerated on board, and the visceral organs were promptly fixed in 10 % neutral-buffered formalin. After landing, the organs were sectioned and processed within 24 h of fixation at the Department of Veterinary Medicine, University of Sassari. Several 1 cm thick rings were excised from the esophagus of each specimen, rinsed several times with chilled 70 % ethanol, and sent to the University of Ferrara for embedding in paraffin wax [11,12]. Sections from paraffin-embedded samples were stained with hematoxylin and eosin, Giemsa, and Sirius red, and images were captured using a Nikon microscope (ECLIPSE 80i; Nikon, Tokyo, Japan).

Sections from paraffin-embedded samples were sent to the University of Milan for immunohistochemical (IHC) testing. Ten antibodies (Table 1) were applied to the esophageal sections, according to a standard laboratory protocol. Briefly, the sections were rehydrated, washed twice in 1 × phosphate-buffered saline (PBS) pH 7.4 for 2 × 5 min, and treated with 3 % H_2O_2 (Sigma-Aldrich, USA) in PBS for 20 min to block endogenous peroxidase activity. The slides were then washed with PBS, placed in a humid chamber, and covered with 1:20 goat normal serum for 30 min to block non-specific staining. Subsequently, the sections were incubated with polyclonal rabbit or monoclonal mouse antibodies (Table 1) for 24 h at room temperature. According to the recommendations provided by the antibody manufacturer, the sections intended for anti-proliferating cell nuclear antigen (PCNA), tumor necrosis factor-α (TNF-α), inducible nitric oxide synthase (i-NOS), and c-kit protein (CD117) were subjected to antigen retrieval through pretreatment with two microwave cycles (2 × 5 min at 450 W in 0.01 M citrate buffer, pH 6.0). Slides processed with rabbit polyclonal antibodies were washed twice in PBS for 5 min and treated with biotinylated goat anti-rabbit immunoglobulins (Table 1, Vector Lab., USA) diluted 1:200 in PBS for 60 min. The sections incubated with mouse monoclonal antibodies were washed as described above and treated with goat anti-mouse immunoglobulins (Table 1, Vector Lab., USA) diluted 1:200 in PBS for 60 min. All slides were then washed twice with PBS for 5 min and treated with streptavidin-biotin/horseradish-peroxidase complex (Vectastain® ABC Kit, Vector Labs., USA) for 60 min. After a brief wash in PBS, the slides were incubated with freshly prepared 0.04 % diaminobenzidine tetrahydrochloride (DAB; Sigma-Aldrich, St. Louis, MO, USA) solution in PBS containing 0.1 ml of 1 % H_2O_2 for 7–14 min, and counterstained with Mayer's hematoxylin. The slides were dehydrated and mounted using Eukitt (Sigma-Aldrich, USA). Negative controls (Fig. S1) were established by (1) incubation with PBS instead of the primary antibody, (2) treatment with PBS instead of the secondary antibody, (3) pre-adsorption of certain antibodies with their corresponding blocking molecules (Table 2), and (4) for the anti-histamine, -lysozyme, and -serotonin antibodies, the use of two antibodies targeting distinct epitopes [13]. Sections of mammalian tissues served as positive controls and yielded the expected results. Images of the experiments were captured using a B-1000FL-HBO microscope (Optika, Bergamo, Italy) equipped with a digital camera (C-P20CC, 20 MP, Optika) and image analysis software (Proview v. x64, Optika).

Table 1
Antibodies used in this study, their specificity, working dilution, source and code.

Mouse monoclonal antibody anti-	Source	Code	Isotype	Working dilution
PCNA[a]	Dako (now part of Agilent Technologies, Santa Clara, CA, USA)	M0879	IgG2a	1:100
CD117 (c-kit protein)[a]	Dako (now part of Agilent Technologies, Santa Clara, CA, USA)	A4502	IgG1	1:50
Lysozyme	Santa Cruz Biotechnology, Inc., Santa Cruz, CA, USA	sc-518012	IgG1	1:50
i-NOS[a]	Santa Cruz Biotechnology, Inc., Santa Cruz, CA, USA	sc-7271	IgG1	1:50
Rabbit polyclonal antibody anti-	**Source**	**Code**	**Isotype**	**Working dilution**
Histamine	Novus Biologicals, Centennial, CO, USA	NBP2-45266	IgG	1:50
Histamine	Sigma-Aldrich, Saint Louis, MO, USA	H7403	IgG	1:50
Lysozyme	Dako (now part of Agilent Technologies, Santa Clara, CA, USA)	A0099	IgG	1:100
Serotonin	Novus Biologicals, Centennial, CO, USA	NB100-65218	IgG	1:100
Serotonin	Sigma-Aldrich, Saint Louis, MO, USA	S5545	WA	1:50
TNF-α[a]	Abcam, Cambridge, UK	ab6671	IgG	1:50
Goat biotinylated anti-				
Mouse immunoglobulinG	Vector Labs, Burlingame, CA, USA	BA-9200	IgG	1:200
	Used for indirect immunochemistry against mouse monoclonal antibodies			
Rabbit immunoglobulinG	Vector Labs, Burlingame, CA, USA	BA-1000	IgG	1:200
	Used for indirect immunochemistry against rabbit polyclonal antibodies			

[a] Antigen retrivial: 2 × 5min in citrate buffer pH6.0 in microwave owen at 450–500W; PCNA: proliferating cell nuclear antigen; CD117: cluster of differentiation 117; i-NOS: inducible-nitric oxide synthase; TNF-α: tumor necrosis factor-α. IgG: immunoglobulin G; IgG1: Immunoglobulin G subclasses 1; IgG2a: immunoglobulin G subclasses 2a; WA: whole antiserum.

Table 2
Blocking molecules used for the antibody pre-adsorption test.

Blocking molecules	Source	Code
Histamine	Sigma-Aldrich, Saint Louis, MO, USA	59964
Serotonin	Sigma-Aldrich, Saint Louis, MO, USA	14927
i-NOS	Santa Cruz Biotechnology, Inc., Santa Cruz, CA, USA	sc-7271 P
TNF-α	Abcam, Cambridge, UK	ab259410

i-NOS: inducible-nitric oxide synthase; TNF-α: tumor necrosis factor-α.

Moreover, the western blot molecular analyses were used for the validation of the antibodies anti-i-NOS, and -TNF-α, for which there are different isoforms in elasmobranchs compared to humans. A section (8 μm) from each catshark and ray was processed for the protein extraction method and the western blot analysis according to the protocol by Mansour et al. [14]. Briefly, the deparaffinization process was performed with hot distilled water (approx. 95 °C). The paraffin was washed off placing the slide three times for 3min in clean beaker containing distilled water on temperature controlled hot plate and heat until temperature 90–95 °C. Then, the tissue specimen was scraped off the slide using a clean cell scraper and transferred into a clean 1.5 ml tube thereafter. A volume of 250 μl of lysis buffer (50 mM Tris-HCL pH7.4, 1 % Triton X-100, 0.2 % Sodium deoxycolate, 1 mM disodium EDTA, 0.2 % SDS) containing the PMSF solution was added to the 1.5 ml microcentrifuge tube. The sample was homogenized using ultrasonic sonicator and then incubated again at 100 °C for 10 min. After 1h incubation at 4 °C, the sample was centrifuged at 2300g for 5 min at 4 °C, and the supernatant was collected into a new clean 1.5 ml microcentrifuge tube. The concentration of total protein isolated from tissue sections was quantified using Lowry assay. Western blot was performed to validate the protein expression extracted from the catshark and ray tissues. Protein extracts were separated on SDS denaturing 12 % polyacrylamide gel and electrophoretically transferred to polyvinylidene difluoride membranes (PVDF). The membranes were blocked with 5 % milk for 1 h for i-NOS2 analysis and 5 % BSA for TNF-α, washed, and then probed with primary antibodies raised against i-NOS2 and TNF-α proteins at 4 °C overnight. Finally, the membranes were treated with HRP-coupled secondary antibodies for 1 h, and the membranes were then washed three times with TBST (1x) for 10 min each thereafter. Protein detection is revealed using the ECL detection kit (Euroclone). Blot images were obtained with the Image Studio Software (Li-COR imaging system). The protein expression for the two antibodies is shown in Fig. S2.

The average areas occupied by immunoreactive granulocytes were obtained as follows. Five randomly selected and homogeneous microscopic images from four specimens each of ray and catshark were used for the quantification of immunoreactive cells. Twenty images were obtained using the 100 × objective (NA 1.30, Optika) of the microscope. For each antibody used, the mean percentage of the area occupied by immunoreactive cells was calculated from the 20 images using the open-source software ImageJ 1.52p (Table 3) and accompanied by the standard error (S.E.). The procedure employed for quantification has been reported in our previous study [6]. To confirm the results obtained from images captured at 100 × magnification, the procedure was applied to microscopic images obtained using a 40 × objective (NA 0.75, Optika). Tables S1 and S2 report the comparison of the mean areas obtained using the two microscopic objectives. Statistical analyses using the Mann–Whitney test demonstrate the similarity between the two sets of measurements (Tables S1 and S2). The comparison between the mean percentage area occupied by immunoreactive cells for each antibody in the two species was performed using the Mann–Whitney test (Table 3).

Datasets concerning the immune markers identified in the LO of *G. melastomus* [6] alongside data from the present study on the LO of *S. canicula* and *R. clavata*, were compared using the Kruskal–Wallis test with Dunn's multiple comparison test (Table 4). Given that the data did not satisfy the assumptions of normality and homogeneity of variances, non-parametric statistical methods, specifically the Mann–Whitney and Kruskal–Wallis tests, were used. All statistical analyses were conducted using Prism 5 for Windows, version 5.03.

For the evaluation of the percentage of PCNA-positive nuclei, we followed the method reported by Bosi et al. [6]. Sections from each ray and catshark specimen were treated with anti-PCNA antibody (Table 1). Slides were mounted using Vectashield mounting medium containing DAPI (Vector Labs; H-1200). Five microscopic images were acquired from ten specimens of ray and ten specimens of catshark using a confocal laser scanning microscope FV300 (Olympus, Tokyo, Japan) equipped with Fluoview v.5.0 software (Olympus). For each species, the 60 × oil objective (n.a. 1.40, Olympus) was used to acquire the 50 pairs of images for anti-PCNA and DAPI. Fig. S3A and S3B show examples of images obtained using anti-PCNA antibody and DAPI, respectively. After processing with ImageJ 1.54f software [6], the resulting images are shown in Fig. S3C and S3D. For each image pair, the percentage of PCNA-positive nuclei was calculated relative to the total number of DAPI-positive nuclei. The mean % ± S.E., corresponding to the mean percentage of proliferating cells, was obtained from 50 datasets (five images × ten specimens) from each of the two species studied.

3. Results

In both *R. clavata* and *S. canicula*, the LO contained a high number of packed leukocytes forming lobes interspersed with irregular venous lacunae (Fig. 1A). The lobes consisted of heterogeneous clusters of leukocytes arterioles and venules (Fig. 1A, B, and 2). In the LO parenchyma of the ray, several eosinophil structures similar to Hassall-like corpuscles were observed (Fig. 1B). Sirius red and Alcian blue/periodic acid-Schiff staining excluded the presence of collagen and glycoconjugates in the Hassall-like structures (Fig. 1C and D). In the LO of the ray and catshark, FEGs and CEGs, lymphocytes, neutrophils, and

Table 3
Comparison between the mean percentage of the area occupied by immunoreactive cells in the Leydig organ of *Raja clavata* and *Scyliorhinus canicula*. The mean was calculated on microscopic images (n = 20) acquired with 100 × objectives. The mean percent value ± standard error (S.E.), and the minimum and maximum percent are reported for each used antibody. The Mann–Whitney test is performed to establish the similarity between the two sets of values.

Antibody anti-	Mean % area ±S.E.		Mann-Whitney test (U)	p
	R. clavata	*S. canicula*		
CD117 (c-kit) (min-max)	14.7 ± 0.9 (7.4–20.5)	13.0 ± 0.5 (7.5–15.9)	148.0	0.1632
Serotonin (min-max)	11.9 ± 0.7 (5.9–15.8)	10.4 ± 0.6 (6.4–15.0)	138.0	0.0961
Histamine (min-max)	16.6 ± 0.8 (11.3–23.3)	14.4 ± 0.7 (9.5–19.9)	133.5	0.0833
Lysozyme (min-max)	16.5 ± 0.4 (13.5–19.0)	15.7 ± 0.7 (10.7–21.3)	166.5	0.3718
TNF-α (min-max)	13.8 ± 0.4 (11.1–16.8)	12.8 ± 0.6 (8.7–16.7)	151.5	0.1940
i-NOS (min-max)	8.8 ± 0.3 (7.1–10.9)	10.1 ± 0.5 (7.2–14.0)	154.5	0.2230

CD117: cluster of differentiation 117; i-NOS: inducible-nitric oxide synthase; TNF-α: tumor necrosis factor-α; p: probability value.

Table 4
Comparison between the mean percentage of the area occupied by immunoreactive cells in the Leydig organ of *Raja clavata*, *Scyliorhinus canicula,* and *Galeus melastomus*. The mean percent value ± standard error (S.E.) was calculated on microscopic images (n = 20) acquired with 100x objectives for each used antibody. Data sets for *G. melastomus* were obtained from our previous survey [6]. The Kruskall-Wallis test was performed to establish the similarity between the three sets of values.

Antibody anti-	Mean % area ±S.E.			Kruskall-Wallis test	p
	R. clavata	*S. canicula*	*G. melastomus*[a]		
CD117 (c-kit)	14.7 ± 0.9	13.0 ± 0.5	14.8 ± 0.7	2.204	0.3322
Serotonin	11.9 ± 0.7	10.4 ± 0.6	18.5 ± 0.5*	37.460	<0.0500
Histamine	16.6 ± 0.8	14.4 ± 0.7	12.5 ± 1.1*	10.720	<0.0500
Lysozyme	16.5 ± 0.4	15.7 ± 0.7	15.3 ± 0.8	1.295	0.5235
TNF-α	13.8 ± 0.4	12.8 ± 0.6	11.2 ± 0.8*	8.002	<0.0500
i-NOS	8.8 ± 0.3	10.1 ± 0.5	11.5 ± 0.9	4.123	0.1273

*p < 0.05, by Dunn's multiple comparison test.
[a] Values from Bosi et al., 2025 [6]; CD117: cluster of differentiation 117; i-NOS: inducible-nitric oxide synthase; TNF-α: tumor necrosis factor-α; p: probability value.

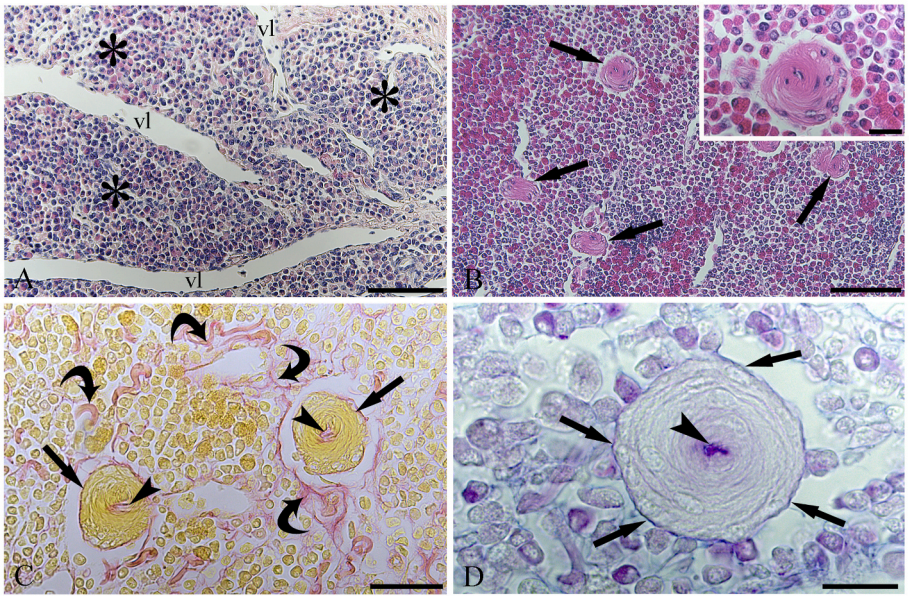

Fig. 1. Histology of the Leydig organ (LO) of *Scyliorhinus canicula* (*Sc*) and *Raja clavata* (*Rc*). (A) The LO of *Sc* shows compact clusters of leukocytes (asterisks) separated by venous lacunae (vl). Hematoxylin and eosin, scale bar 100 μm. (B) High number of leukocytes in the LO of *Rc* with several Hassall-like corpuscles (arrows) interspersed in the parenchyma. The insert shows high magnification of a Hassall-like corpuscle. Hematoxylin and eosin, scale bars 100 μm, insert 20 μm. (C) A network of thin red collagen fibers (curved arrows) supports the clusters of leukocytes in the LO of *Rc*. Note two unstained Hassall-like corpuscles (arrows), with only the cores stained red (arrowheads). Sirius red, scale bar 50 μm. (D) High magnification of a Hassall-like corpuscle in the LO of *Rc*. A thin alcianophilic layer surrounds the concentric structure (arrows), and the core shows a violet color, indicating positivity for both Alcian blue and periodic acid-Schiff (arrowhead). Most of the corpuscle appears unstained. Alcian blue/periodic acid-Schiff, scale bar 20 μm. (For interpretation of the references to color in this figure legend, the reader is referred to the Web version of this article.)

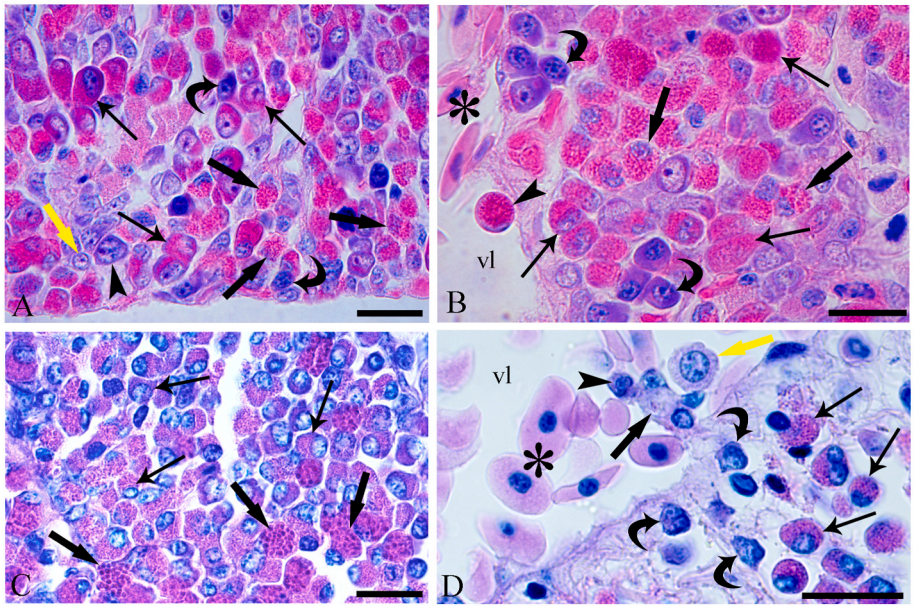

Fig. 2. Giemsa staining of the Leydig organ (LO) of *Scyliorhinus canicula* (*Sc*) and *Raja clavata* (*Rc*). (A) In the LO of *Sc*, numerous fine eosinophilic granulocytes (FEGs, thin arrows) and coarse eosinophilic granulocytes (CEGs, thick arrows) are observed. Curved arrows show very few neutrophils, and the arrowhead and yellow arrow indicate a blast cell and lymphoblast/cyte, respectively. (B) Magnification of an LO section of *Sc* close to a venous lacuna (vl) shows a region with FEGs (thin arrows), CEGs (thick arrows), and neutrophils (curved arrows). Note the erythrocytes (asterisk) in the lacuna, and a granulocyte (arrowhead) leaving the parenchyma to enter the bloodstream. (C) Section of the LO of *Rc* with clusters of FEGs (thin arrows) and CEGs (thick arrows). (D) In a region of the *Rc* LO near a vl, some FEGs (thin arrows) and neutrophils (curved arrows) are visible in the parenchyma. In the vl, a probable macrophage (thick arrow) is close to a lymphocyte-like cell (arrowhead), plasma cell (yellow arrow), and several erythrocytes (asterisk). Scale bars 20 μm. (For interpretation of the references to color in this figure legend, the reader is referred to the Web version of this article.)

undifferentiated progenitors were observed (Fig. 2). Presumably differentiated leukocytes were visible in the venous lacunae (Fig. 2B–D).

In the LO of *R. clavata*, 44.0 ± 1.1 % (mean ± S.E.) of total cells were positive for anti-PCNA, with a percentage range of 28.4–67.0 %. The proportion of total cells immunoreactive to anti-PCNA was 44.9 ± 0.8 % in the LO of *S. canicula*, ranging from 31.5 % to 63.8 %. The cells positive

for anti-CD117 covered an average area of 14.7 ± 0.9 % and 13.0 ± 0.5 % in the LO of the ray and catshark, respectively (Table 3).

The CEGs were immunoreactive to the anti-serotonin antibodies used in the LO of both species (Fig. 3A and B), with average occupied areas of 11.9 ± 0.7 % in the ray and 10.4 ± 0.6 % in the catshark (Table 3). The CEGs were also positive to the anti-histamine antibodies (Fig. 3C and D), and the mean percentage areas of reactive cells were 16.6 ± 0.8 % and 14.4 ± 0.7 % in *R. clavata* and *S. canicula*, respectively (Table 3). Several cells were immunoreactive to the anti-lysozyme antibodies tested (Fig. 4A and B), covering mean areas of 16.5 ± 0.4 % and 15.7 ± 0.7 % in the LO sections of *R. clavata* and *S. canicula*, respectively (Table 3). In addition, the LO of the catshark exhibited FEGs that were positive to anti-TNF-α, and anti-i-NOS (Fig. 4C–E) occupying average areas of 12.8 ± 0.6 %, and 10.1 ± 0.5 %, respectively (Table 3). In the LO of the ray, several FEGs were immunoreactive to anti-TNF-α (Fig. 4C), and anti-i-NOS (Fig. 4D and E). The mean area covered by immunoreactive cells was 13.8 ± 0.4 % for anti-TNF-α, and 8.8 ± 0.3 % for i-NOS (Table 3). The Western Blot analysis on proteins extracted from sections of catshark and ray tissues validates the immunohistochemical results for antibodies anti- TNF-α and -i-NOS (Fig. S2). No CEGs exhibited immunoreactivity to anti-lysozyme or anti-i-NOS (Fig. 4F) in the LO of the ray or catshark.

Statistical analysis indicated a significant difference in the percentage area occupied by granulocytes immunoreactive to histamine, serotonin, and TNF-α between the two species in the present study and *G. melastomus* (Table 4).

4. Discussion

Sharks and rays diverged from a common ancestor of other cartilaginous fish approximately 420 million years ago [15]. Elasmobranchs represent an important research model for evolutionary investigations of several vertebrate characteristics that first appeared in sharks and rays or were found only in this taxon [15]. The LO is an elasmobranch-specific leukopoietic organ associated with the esophagus and there is a lack of LO homologs in amniotes [16]. Studies on the structure of vertebrate lymphoid organs from a phylogenetic perspective will help us understand the sequence of steps in the evolution of their immune systems [17,18].

The LO histology in *S. canicula* and *R. clavata* resembles that of other studied elasmobranch species [4,6,19]. Hematoxylin and eosin and Giemsa staining showed that the LO of the small-spotted catshark and thornback ray differed owing to the tinctorial properties of their cells, a finding similar to that reported for other elasmobranch species [10]. In this study, several Hassall-like corpuscles were observed exclusively in the parenchyma of the ray LO, and the components of these structures lacked both collagen fibers and glycoconjugate molecules. Hassall bodies have been found in the thymus of several teleosts, but not in all species [18,20]. In the thymus of starlet, *Acipenser ruthenus*, Hassall-like corpuscles were immunoreactive to an anti-cytokeratin antibody [21], and the same result was reported earlier for the lungfish thymus [22]. In amniotes, Hassall's bodies are multilayered epithelial cell structures related to the differentiation of medullary thymic epithelial cells [18]. In teleosts, the occurrence and number of Hassall-like bodies appear to be variable, and there is a dearth of information on these structures [18].

This study showed that approximately 44 % of cells in the LO of both species were in DNA synthesis activity, as confirmed by immunofluorescence with an anti-PCNA antibody. The gene sequence and functions of PCNA are considerably conserved among eukaryotes, and an increase of cell number expressing PCNA is a signal of marked rise in the rate of cellular division [23]. This result aligns well with the percentage of proliferating cells previously observed in the LO of *G. melastomus* [6]. In histological sections of the LO of the small-spotted catshark and thornback ray, a mean area of 13–14 % was occupied by cells in a differentiation stage, as shown by the immunoreaction with anti-CD117 (KIT receptor tyrosine kinase). CD117 is a transmembrane receptor expressed in cells during differentiation/activation [24,25]. A similar mean percentage area of cells immunoreactive to anti-CD117 was found in the LO of the blackmouth catshark [6]. Our data on anti-PCNA and anti-CD117 are consistent with the statement that the elasmobranch LO is the site of proliferation and activation of immune cells [2,6,19].

Two types of granulocytes, FEGs and CEGs, were the most prevalent cell types in the LO of both species. Other cell types encountered included neutrophils, lymphoblastoid cells packed in clusters, and

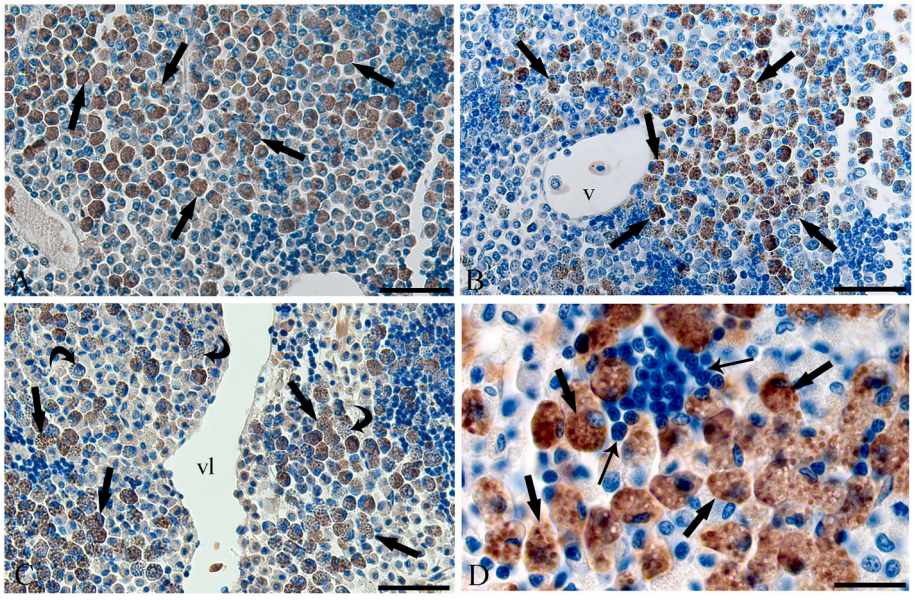

Fig. 3. Immunohistochemistry of granulocytes in the Leydig organ (LO) of *Scyliorhinus canicula* (*Sc*) and *Raja clavata* (*Rc*). (A) In the LO of *Rc*, numerous granulocytes with coarse granules (CEGs, thick arrows) were immunoreactive to anti-serotonin antibody. Scale bar 50 μm. (B) The LO of *Sc* shows several CEGs (thick arrows) reactive to anti-serotonin, most of which are located near a venule (v). Scale bar 50 μm. (C) Anti-histamine antibody is detected by CEGs (thick arrows) in the LO of *Rc*. Not all CEGs are positive to the antibody (curved arrows). vl: venous lacuna. Scale bar 50 μm. (D) High magnification shows the CEGs (thick arrows) immunoreactive to anti-histamine in the LO of *Rc*. The thin arrows indicate a lymphoblast/cyte cluster. Scale bar 20 μm.

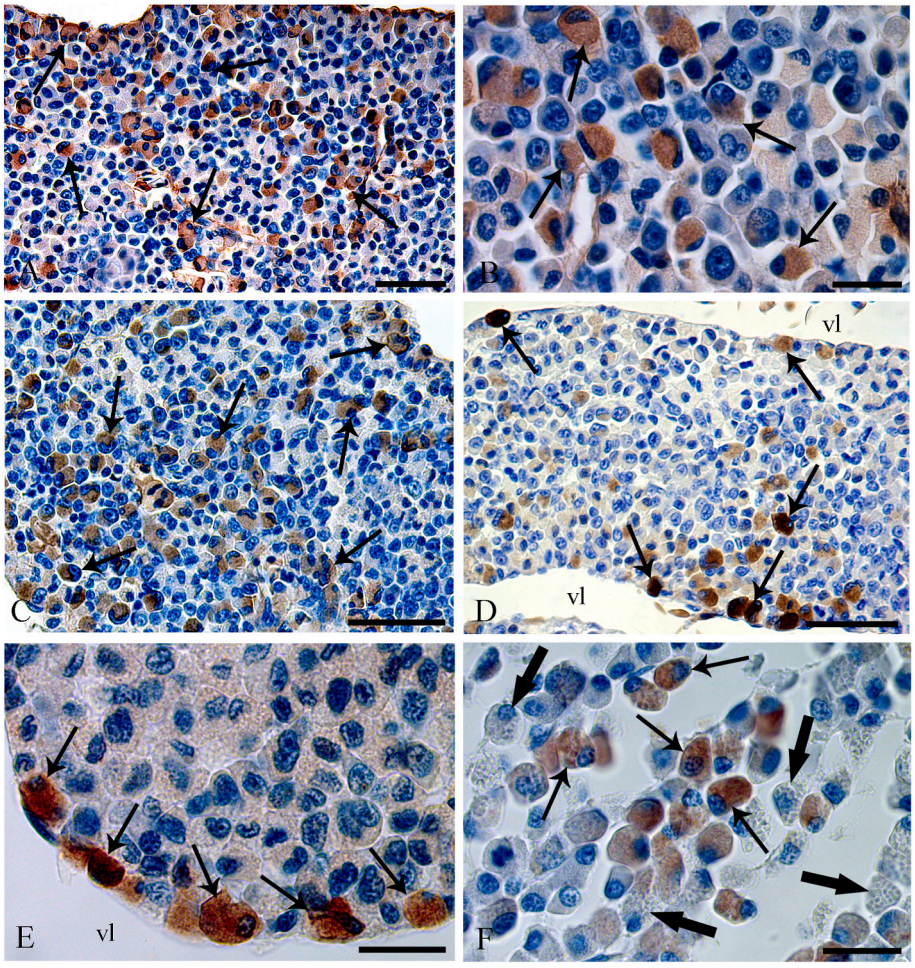

Fig. 4. Immunohistochemistry of granulocytes in the Leydig organ (LO) of *Scyliorhinus canicula* (*Sc*) and *Raja clavata* (*Rc*). (A) Several granulocytes with fine granules (FEGs, thin arrows) immunoreactive to anti-lysozyme antibody in the LO of *Sc*. Scale bar 50 μm. (B) High magnification shows FEGs (thin arrows) positive to anti-lysozyme in the LO of *Rc*. Scale bar 20 μm. (C) Numerous FEGs (thin arrows) are immunoreactive to anti-TNF-α antibody in the LO of *Rc*. Scale bar 50 μm. (D) In the LO of *Sc*, the FEGs (thin arrows) positive to anti-i-NOS antibody are mainly close to vl. Scale bar 50 μm. (E) High magnification shows some FEGs (thin arrows) immunoreactive to anti-i-NOS antibody near to a vl in the LO of *Sc*. Scale bar 20 μm. (F) Some FEGs immunoreactive to i-NOS (thin arrows) in a loose region of the LO parenchyma of *Rc*. Note the unstained granulocytes with coarse granules (thick arrows). Scale bar 20 μm.

rarely, basophils. Some leukocytes were found in the blood vessels and venous lacunae; presumably, these differentiated cells leave the LO parenchyma and migrate to the tissues where they are needed [6].

In differentiating cells, protein synthesis drives the appearance and maturation of cytoplasmic specific granules of each granulocyte type [3]. The composition of cytoplasmic granules can be investigated using immunohistochemical analysis. Despite the lack of specific cell markers for elasmobranch leukocytes, several studies have used antibodies produced for mammals and teleosts [26–28]. The implementation of stringent control protocols, incubation of tissue sections with various antibodies targeting distinct epitopes of the target molecules, detection of an antibody signal in compatible cells or cell structures, and molecular procedures to validate antibodies against proteins derived from multiple genes in evolutionary distant organisms, constitute definitive evidence of cross-reactivity [6,11,28–30].

The biogenic amines serotonin and histamine were detected using immunohistochemical tests in the granulocytes of the LO of the small-spotted catshark and thornback ray, showing a comparable mean percentage area of approximately 10–12 % for serotonin and 14.5–16.5 % for histamine. The CEGs were positive to anti-histamine and anti-serotonin, as was also observed in the LO of *G. melastomus* [6]. These two small amines are widely expressed in plants and animals [31–33]. Statistical analysis showed a significant difference in the percentage area occupied by serotonin- and histamine-reactive granulocytes when the data for the two species in this study were compared with those obtained for the blackmouth catshark. These differences were most likely due to species-specific patterns, as reported for granulocyte morphology and content in other elasmobranch species [2].

Lysozyme is the most important enzyme produced by the animal innate immune system and is stored in macrophages and neutrophils [34,35]. Lysozyme has been demonstrated in immune cells in the lympho-myeloid tissues of some elasmobranch species and in the spiral intestine of *R. clavata* and *G. melastomus* [11,29,36]. Approximately 16.5 % and 15.7 % of the LO histological sections of the thornback ray and small-spotted catshark, respectively, were immunoreactive to the two anti-lysozyme antibodies used. In the LO histological sections of *G. melastomus*, the area positive for lysozyme was 15.3 % [6]. The area occupied by lysozyme-reactive cells was similar in the LO of the three elasmobranch species. Another important antimicrobial enzyme secreted by mast cells, macrophages, and neutrophils is i-NOS [12,37]. The amino acid L-arginine is rapidly converted to L-citrulline and nitric oxide (NO) through the catalyst i-NOS [38]. Gaseous NO generated by immune cells induces apoptosis in nearby cells and damages pathogens [12,39]. The anti-i-NOS antibody revealed no difference in the areas of the LO histological sections occupied by the immunoreactive cells in the small-spotted catshark and thornback ray. Granulocytes positive for

anti-i-NOS antibody were often located at the border of the parenchymatic lobes, close to the venous lacunae. In the LO of the blackmouth catshark, a similar area was positive to anti-i-NOS [6]. NO in the immune system promotes a local non-specific inflammatory response against pathogens [40].

The cytokine TNF-α is a small peptide secreted by fish neutrophils and macrophages that is involved in immune function modulation [29,41–44]. It was not possible to identify the exact TNF paralog detected by the used antibody anti-TNF-α. However, the granulocytes immunoreactivity to the anti-TNF-α, validated by western blot analysis, revealed the presence of a TNF-like protein in the LO of the two studied species. Approximately 12.8–13.8 % of the LO histological sections of the two species studied were positive to anti- TNF-α. In the LO of *G. melastomus*, granulocytes positive to anti-TNF-α occupied an area equal to 11.2 % [6]. This indicates a significant difference in the area of the LO immunoreactive to anti-TNF-α between the two species in the present study and the blackmouth catshark. TNF-α is highly expressed during inflammatory responses [29,44]. Consequently, it is reasonable to hypothesize that the observed differences may be attributed to the physiological state of the shark and ray specimens and species-specific differences [2]. The areas of the LO histological sections occupied by granulocytes immunoreactive to anti-CD117, -lysozyme, and i-NOS did not differ among the three elasmobranch species. In the LO of the small-spotted catshark and thornback ray, the immunohistochemical analyses confirmed the presence of the immune markers detected in the LO of *G. melastomus* [6]. As observed in the LO of the blackmouth catshark [6], two primary cell lineages were identified in the LO of *S. canicula* and *R. clavata*. These include a macrophage lineage represented by granulocytes with fine granules containing lysozyme, i-NOS, and TNF-α, and a mast cell lineage of granulocytes with coarse granules containing serotonin and histamine.

The LO of elasmobranchs serves as a site for the proliferation and differentiation of granulocytes and plays a role in immune defense mechanisms against pathogens [2,6]. Studies on the immune systems of elasmobranchs represent a recent and rapidly growing field of investigation [15,43,45,46]. This interest is partly driven by the limited understanding of elasmobranch diseases in nature [47] and the identification of several molecules from shark tissues with active pharmacological properties that are effective against various human diseases, including cancer [48,49]. It has been suggested that anticancer peptides derived from elasmobranchs offer several advantages over conventional chemotherapeutic drugs [49,50]. The data presented in this article constitute a first attempt to characterize and quantify granulocytes in the LO of *S. canicula* and *R. clavata* with the aim of expanding the knowledge on this peculiar immunological organ. These exploratory results partially fill an information gap and hopefully provide a basis for further research.

CRediT authorship contribution statement

Giampaolo Bosi: Conceptualization, Methodology, Investigation, Data curation, Writing-original draft. Paolo Merella: Conceptualization, Data curation, Validation. Emanuela Franchella: Investigation, Data curation. Bahram Sayyaf Dezfuli: Conceptualization, Methodology, Investigation, Data curation, Writing - review & editing, Resources, Funding acquisition. Stefania Zava: Methodology, Investigation, Data curation. Paola Antonia Corsetto: Methodology, Investigation, Data curation, Luisa Giari: Conceptualization, Visualization, Data curation, Supervision, Writing – review & editing, Funding acquisition.

Funding

This work was supported by local grants from the University of Ferrara to Bahram Sayyaf Dezfuli and Luisa Giari (grant number FAR 2024).

Declaration of competing interest

All authors confirm that they have no interests to declare.

Acknowledgements

Special thanks to the staff of the fishing boat Firm Rum belonging to Antonio & Umberto S.N.C. for providing the samples. Thanks are due to Giovanni Bernacchia from University of Ferrara for the critical revision of the revised draft.

Appendix A. Supplementary data

Supplementary data to this article can be found online at https://doi.org/10.1016/j.fsi.2025.111095.

Data availability

Data will be made available on request.

References

[1] C.D. Mitchell, M.F. Criscitiello, M.F, Comparative study of cartilaginous fish divulges insights into the early evolution of primary, secondary and mucosal lymphoid tissue architecture, Fish Shellfish Immunol. 107 (2020) 435–443, https://doi.org/10.1016/j.fsi.2020.11.006.
[2] A.G. Zapata, M. Torroba, R. Sacedón, A. Varas, A. Vicente, Structure of the lymphoid organs of elasmobranchs, J. Exp. Zool. 275 (1996) 125–143, https://doi.org/10.1002/(SICI)1097-010X(19960601/15)275:2/3<125::AID-JEZ6>3.0.CO;2-F.
[3] A. Zapata, Ultrastructure of elasmobranch lymphoid tissue. 2. Leydig's and epigonal organs, Dev. Comp. Immunol. 5 (1981) 43–52, https://doi.org/10.1016/S0145-305X(81)80006-7.
[4] A. Mattisson, R. Fänge, The cellular structure of the leydig organ in the shark *Etmopterus spinax* L, Biol. Bull. 162 (1982) 182–194.
[5] R. Fänge, A. Mattisson, The lymphomyeloid (hemopoietic) system of the Atlantic nurse shark *Ginglymostnmu cirrutum*, Biol. Bull. 160 (1981) 240–249.
[6] G. Bosi, P. Merella, E. Franchella, B. Sayyaf Dezfuli, L. Giari, The leydig organ of elasmobranchs: shed light on an active and mysterious defense center with immunological characterization of its cells, Tissue Cell 93 (2025) 102755, https://doi.org/10.1016/j.tice.2025.102755.
[7] P.M. Hine, J.M. Wain, The enzyme cytochemistry and composition of elasmobranch granulocytes, J. Fish. Biol. 30 (1987) 465–475, https://doi.org/10.1111/j.1095-8649.1987.tb05770.x.
[8] P.M. Hine, J.M. Wain, Composition and ultrastructure of elasmobranch granulocytes. III. Sharks (Lamniformes), J. Fish. Biol. 30 (1987) 567–576, https://doi.org/10.1111/j.1095-8649.1987.tb05784.x.
[9] P.M. Hine, The granulocytes of fish, Fish Shellfish Immunol. 2 (1992) 79–98, https://doi.org/10.1016/S1050-4648(05)80038-5.
[10] H.S. Carmezim, R. Marcos, There is plenty more fish nomenclature in the sea: the elasmobranch granulocytes, Vet. Clin. Pathol. 49 (2020) 196–197, https://doi.org/10.1111/vcp.12875.
[11] G. Bosi, B. Sayyaf Dezfuli, P. Merella, L. Giari, Immune cells in the spiral intestine of Blackmouth catshark, *Galeus melastomus*: new insights into ancient gut defenders, Egyp. J. Aquat. Res. 50 (2024) 566–576, https://doi.org/10.1016/j.ejar.2024.10.002.
[12] B. Sayyaf Dezfuli, F. Pironi, G. Castaldelli, L. Giari, M. Lanzoni, K. Buchmann, P. W. Kania, G. Bosi, *Anguilla Anguilla* vs *Contracaecum rudolphii*: granuloma allows host tolerance and parasite survival, Aquaculture 591 (2024) 741138, https://doi.org/10.1016/j.aquaculture.2024.741138.
[13] J.D. Webster, M. Solon, K.N. Gibson-Corley, Validating immunohistochemistry assay specificity in investigative studies: considerations for a weight of evidence approach, Vet. Pathol. 58 (2021) 829–840, https://doi.org/10.1177/0300985820960132.
[14] A.G. Mansour, P. Abou-Khalil, N. Bejjani, R. Chatila, C. Dagher-Hamalian, W. H. Faour, An optimized xylene-free protein extraction method adapted to formalin-fixed paraffin embedded tissue sections for western blot analysis, Histol. Histopathol. 32 (2017) 307–313, https://doi.org/10.14670/HH-11-789, 2017.
[15] H. Dooley, Chondrichthyes: the immune system of cartilaginous fishes, in: E. Cooper (Ed.), Advances in Comparative Immunology, Springer, Cham, 2018, pp. 659–685, https://doi.org/10.1007/978-3-319-76768-0_18.
[16] J.L. Smith, G.C. Schoenwolf, Getting organized: new insights into the organizer of higher vertebrates, Curr. Top. Dev. Biol. 40 (1998) 79–110, https://doi.org/10.1016/S0070-2153(08)60365-8.
[17] T. Boehm, I. Hess, J.B. Swann, Evolution of lymphoid tissues, Trends Immunol. 33 (2012) 315–321, https://doi.org/10.1016/j.it.2012.02.005.
[18] A.G. Zapata, Lympho-hematopoietic microenvironments and fish immune system, Biol. Basel 11 (2022) 747, https://doi.org/10.3390/biology11050747.

[19] F.J. Pacheco, S.O.S. Pacheco, H.R.C. Segreto, R.A. Segreto, M.R.R. Silva, M. I. Egami, Development of granulocytes in haematopoietic tissues of *Rhizoprionodon lalandii*, J. Fish. Biol. 61 (2002) 888–898, https://doi.org/10.1111/j.1095-8649.2002.tb01850.x.

[20] F.A. Vigliano, A.P. Losada, M. Castello, R. Bermudez, M.I. Quiroga, Morphological and immunohistochemical characterisation of the thymus in juvenile turbot (*Psetta maxima*, L.), Cell Tissue Res. 346 (346) (2011) 407–416, https://doi.org/10.1007/s00441-011-1282-7.

[21] E. Salkova, M. Flajshans, C. Steinbach, Immunohistochemical mapping of thymic microenvironment in sterlet (*Acipenser ruthenus*), Vet. Med. 65 (2020) 301–308, https://doi.org/10.17221/181/2019-VETMED.

[22] M.G. Mohammad, S. Chilmonczyk, D. Birch, S. Aladaileh, D. Raftos, J. Joss, Anatomy and cytology of the thymus in juvenile Australian lungfish, *Neoceratodus forsteri*, J. Anat. 211 (2007) 784–797, https://doi.org/10.1111/j.1469-7580.2007.00814.x.

[23] A.Y.H. Leung, J.C.K. Leung, L.Y.Y. Chan, E.S.K. Ma, T.T.F. Kwan, K.N. Lai, A. Meng, R.A. Liang, Proliferating cell nuclear antigen (PCNA) as a proliferative marker during embryonic and adult zebrafish hematopoiesis, Histochem. Cell Biol. 124 (2005) 105–111, https://doi.org/10.1007/s00418-005-0003-2.

[24] M. Miettinen, J. Lasota, Kit (CD117): a review on expression in normal and neoplastic tissues, and mutations and their clinicopathologic correlation, Appl. Immunohistochem. Mol. Morphol. 13 (2005) 205–220, https://doi.org/10.1097/01.pai.0000173054.83414.22.

[25] J.T. Dobson, J. Seibert, E.M. The, S. Da'as, R.B. Fraser, B.H. Paw, T.J. Lin, J. N. Berman, Carboxypeptidase A5 identified a novel mast cell lineage in the zebrafish providing new insight into mast cell fate determination, Blood 112 (2008) 2969–2972, https://doi.org/10.1182/blood-2008-03-145011.

[26] R.T. Pereira, T.R. de Freitas, I.R.C. de Oliveira, L.S. Costa, F.A. Vigliano, P.V. Rosa, Endocrine cells producing peptide hormones in the intestine of Nile tilapia: distribution and effects of feeding and fasting on the cell density, Fish Physiol. Biochem. 43 (2017) 1399–1412, https://doi.org/10.1007/s10695-017-0380-1.

[27] E.R. Lauriano, S. Pergolizzi, M. Aragona, G. Montalbano, M.C. Guerrera, R. Crupi, C. Faggio, G. Capillo, Intestinal immunity of dogfish *Scyliorhinus canicula* spiral valve: a histochemical, immunohistochemical and confocal study, Fish Shellfish Immunol. 87 (2019) 490–498, https://doi.org/10.1016/j.fsi.2019.01.049.

[28] C.A. Manire, A.C. Clarke, D. Wert, J. Landolfi, Lymphosarcoma in a captive bonnethead shark, *Sphyrna tiburo* (L.), J. Fish. Dis. 36 (2013) 437–440, https://doi.org/10.1111/j.1365-2761.2012.01435.x.

[29] B. Sayyaf Dezfuli, M. Manera, G. Bosi, P. Merella, J.A. DePasquale, L. Giari, Intestinal granular cells of a cartilaginous fish, thornback ray *Raja clavata*: morphological characterization and expression of different molecules, Fish Shellfish Immunol. 75 (2018) 172–180, https://doi.org/10.1016/j.fsi.2018.02.019.

[30] K.R. Archer, T. Groll, R.J. Harvey, S.M. Thornton, M.F. Stidworthy, D. Denk, Case series: lymphoid neoplasia in three elasmobranch species, J. Fish. Dis. 46 (2023) 273–279, https://doi.org/10.1111/jfd.13742.

[31] R. Gillette, Evolution and function in serotonergic systems, Integr. Comp. Biol. 46 (2006) 838–846, https://doi.org/10.1093/icb/icl024.

[32] R. Pelagio-Flores, R. Ortíz-Castro, A. Méndez-Bravo, L. Macías-Rodríguez, J. López-Bucio, Serotonin, a tryptophan-derived signal conserved in plants and animals, regulates root system architecture probably acting as a natural auxin inhibitor in *Arabidopsis thaliana*, Plant Cell Physiol. 52 (2011) 490–508, https://doi.org/10.1093/pcp/pcr006.

[33] G. Csaba, Biogenic amines at a low level of evolution: production, functions and regulation in the unicellular Tetrahymena, Acta Microbiol. Immunol. Hung. 62 (2015) 93–108, https://doi.org/10.1556/030.62.2015.2.1.

[34] D.M. Irwin, Evolution of the vertebrate goose-type lysozyme gene family, BMC Evol. Biol. 14 (2014) 188, https://doi.org/10.1186/s12862-014-0188-x.

[35] N.C. Smith, M.L. Rise, S.L. Christian, A comparison of the innate and adaptive immune systems in cartilaginous fish, ray-finned fish, and lobe-finned fish, Front. Immunol. 10 (2019) 2292, https://doi.org/10.3389/fimmu.2019.02292.

[36] N. Hinds Vaughan, S.L. Smith, Isolation and characterization of a c-type lysozyme from the nurse shark, Fish Shellfish Immunol. 35 (2013) 1824–1828, https://doi.org/10.1016/j.fsi.2013.09.001.

[37] A.P. Losada, R. Bermúdez, L.D. Faílde, M.I. Quiroga, Quantitative and qualitative evaluation of iNOS expression in turbot (*Psetta maxima*) infected with *Enteromyxum scophthalmi*, Fish Shellfish Immunol. 32 (2012) 243–248, https://doi.org/10.1016/j.fsi.2011.11.007.

[38] C.C. Wei, Z.Q. Wang, C. Hemann, R. Hille, D.J. Stuehr, A tetrahydrobiopterin radical forms and then becomes reduced during Nω-hydroxyarginine oxidation by nitric-oxide synthase, J. Biol. Chem. 278 (2003) 46668–46673, https://doi.org/10.1074/jbc.M307682200.

[39] S. Torrecillas, M.J. Caballero, D. Mompel, D. Montero, M.J. Zamorano, L. Robaina, F. Rivero-Ramírez, V. Karalazos, S. Kaushik, M. Izquierdo, Disease resistance and response against *Vibrio anguillarum* intestinal infection in European seabass (*Dicentrarchus labrax*) fed low fish meal and fish oil diets, Fish Shellfish Immunol. 67 (2017) 302–311, https://doi.org/10.1016/j.fsi.2017.06.022.

[40] E.U. Uehara, B.D. Shida, C.A. de Brito, Role of nitric oxide in immune responses against viruses: beyond microbicidal activity, Inflamm. Res. 64 (2015) 845–852, https://doi.org/10.1007/s00011-015-0857-2.

[41] P. Ronza, A.P. Losada, A. Villamarın, R. Bermudez, M.I. Quiroga, Immunolocalization of tumor necrosis factor alpha in turbot (*Scophthalmus maximus*, L.) tissues, Fish Shellfish Immunol. 45 (2015) 470–476, https://doi.org/10.1016/j.fsi.2015.04.032.

[42] B. Sayyaf Dezfuli, G. Castaldelli, R. Tomaini, M. Manera, J.A. DePasquale, G. Bosi, Challenge for macrophages and mast cells of *Chelon ramada* to counter an intestinal microparasite, *Myxobolus mugchelo* (Myxozoa), Dis. Aquat. Organ. 138 (2020) 171–183, https://doi.org/10.3354/dao03459.

[43] K.B. Carlson, C. Nguyen, D.J. Wcisel, J.A. Yoder, A. Dornburg, Ancient fish lineages illuminate toll-like receptor diversification in early vertebrate evolution, Immunogenetics 75 (2023) 465–478, https://doi.org/10.1007/s00251-023-01315-7.

[44] B. Sayyaf Dezfuli, L. Giari, M. Lorenzoni, A. Carosi, M. Manera, G. Bosi, Pike intestinal reaction to *Acanthocephalus lucii* (Acanthocephala): immunohistochemical and ultrastructural surveys, Parasites Vectors 11 (2018) 424, https://doi.org/10.1186/s13071-018-3002-6.

[45] A. Veríssimo, L.F.C. Castro, A. Muñoz-Mérida, T. Almeida, A. Gaigher, F. Neves, M. F. Flajnik, Y. Ohta, An ancestral major histocompatibility complex organization in cartilaginous fish: reconstructing MHC origin and evolution, Mol. Biol. Evol. 40 (2023) msad262, https://doi.org/10.1093/molbev/msad262.

[46] C. Gargano, M. Mauro, C. Martino, V. Queiroz, V, A. Vizzini, C. Luparello, R. Badalamenti, F. Bellistrì, A. Cuttitta, H. Kondo, F. Longo, V. Arizza, M. Vazzana, Shark immune system: a review about their immunoglobulin repertoire, Fish Shellfish Immunol. 160 (2025) 110187, https://doi.org/10.1016/j.fsi.2025.110187.

[47] C.A. Luer, C.J. Walsh, Potential human health applications from marine biomedical research with elasmobranch fishes, Fishes 3 (2018) 47, https://doi.org/10.3390/fishes3040047.

[48] C.J. Walsh, C.A. Luer, A.B. Bodine, C.A. Smith, H.L. Cox, D.R. Noyes, M. Gasparetto, Elasmobranch immune cells as a source of novel tumor cell inhibitors: implications for public health, Integr. Comp. Biol. 46 (2006) 1072–1081, https://doi.org/10.1093/icb/icl041.

[49] M. Librizzi, C. Martino, M. Mauro, G. Abruscato, V. Arizza, M. Vazzana, C. Luparello, Natural anticancer peptides from marine animal species: evidence from in vitro cell model systems, Cancers 16 (2023) 36, https://doi.org/10.3390/cancers16010036.

[50] R.K. Chinnadurai, N. Khan, G.K. Meghwanshi, S. Ponne, M. Althobiti, R. Kumar, Current research status of anti-cancer peptides: mechanism of action, production, and clinical applications, Biomed. Pharmacother. 164 (2023) 114996, https://doi.org/10.1016/j.biopha.2023.114996.